Maier-Saupe model for a mixture of uniaxial and biaxial molecules

E. S. Nascimento,[1] E. F. Henriques,[2] A. P. Vieira,[1,*] and S. R. Salinas[1]

[1]*Instituto de Física, Universidade de São Paulo, Caixa Postal 66318, 05314-970 São Paulo, SP, Brazil*

[2]*Instituto de Física e Matemática, Universidade Federal de Pelotas, Caixa Postal 354, 96010-900 Pelotas, RS, Brasil*

(Received 1 July 2015; published 1 December 2015)

We introduce shape variations in a liquid-crystalline system by considering an elementary Maier-Saupe lattice model for a mixture of uniaxial and biaxial molecules. Shape variables are treated in the annealed (thermalized) limit. We analyze the thermodynamic properties of this system in terms of temperature T, concentration c of intrinsically biaxial molecules, and a parameter Δ associated with the degree of biaxiality of the molecules. At the mean-field level, we use standard techniques of statistical mechanics to draw global phase diagrams, which are shown to display a rich structure, including uniaxial and biaxial nematic phases, a reentrant ordered region, and many distinct multicritical points. Also, we use the formalism to write an expansion of the free energy in order to make contact with the Landau–de Gennes theory of nematic phase transitions.

DOI: 10.1103/PhysRevE.92.062503 PACS number(s): 61.30.Cz

I. INTRODUCTION

The characterization of biaxial nematic phases in a number of thermotropic liquid-crystalline systems [1–3] stimulated a revival of interest in the investigation of theoretical models to describe biaxial structures [4]. About 40 years ago, Freiser [5] showed the existence of uniaxial and biaxial nematic phases in a generalization of the mean-field Maier-Saupe theory of the nematic transition with the addition of suitably asymmetric degrees of freedom. A nematic biaxial phase has also been shown to exist in a lattice model with steric interactions between platelets [6] and in a number of calculations for model systems with soft- and hard-core interactions [7–9]. The early experimental results, however, referred to a lyotropic liquid-crystalline mixture [10], which should be better represented by a model of uniaxial nematogenic elements [11,12] and which motivated the use of an elementary version of the Maier-Saupe theory [13–15] to investigate a lattice statistical model for a binary mixture of cylinders and disks. We now propose an extension of this elementary model, along the lines of Freiser's generalization of the Maier-Saupe theory, in order to analyze the global phase diagram of a mixture of uniaxial and biaxial molecules.

In some analytical [16] and numerical [11] calculations, it has been pointed out that shape variations play an important role in the stability of biaxial nematic phases. In spite of the complexity of liquid-crystalline systems, whose complete description may require the introduction of more realistic, and necessarily involved, theoretical models, we believe that there is still room for the investigation of elementary statistical lattice models, with the addition of some ingredients that may be essential to describe the main features of the thermodynamic behavior. Along the lines of Freiser's early work, we then add extra degrees of freedom, of a biaxial nature, to an elementary lattice model, which leads to the definition of a six-state Maier-Saupe (MS6) model. This MS6 model is similar to an earlier proposal by Bocarra and collaborators [7] and may be regarded as a generalization of a previously used three-state Potts model to describe the uniaxial nematic transition [17]. Shape variations are taken into account by introducing a "biaxiality parameter," Δ, and by considering a binary mixture of molecules with $\Delta = 0$ (intrinsically uniaxial molecules) and $\Delta \neq 0$ (intrinsically biaxial molecules). This model system is sufficiently simple to be amenable to detailed statistical mechanics calculations for either quenched [18] or annealed mixtures of molecules. We then carry out calculations to obtain global phase diagrams and write an expansion of the free energy for comparison with the standard form of the phenomenological Landau–de Gennes theory of phase transitions.

This paper is organized as follows. In Sec. II, we define the MS6 model for a binary mixture of molecules and formulate the statistical problem. In Sec. III, we analyze the mean-field equations, draw a number of characteristic phase diagrams, and put the problem in the context of the Landau–de Gennes theory. Section IV is devoted to the final discussion and to some conclusions.

II. THE SIX-STATE MAIER–SAUPE MODEL

The standard formulations of the Maier–Saupe theory of nematic phase transitions [19] can be described in terms of the Hamiltonian

$$\mathcal{H} = -\epsilon \sum_{(i,j)} \sum_{\alpha,\beta=1,2,3} \Omega_i^{\alpha\beta}\, \Omega_j^{\alpha\beta}, \tag{1}$$

where ϵ is a positive parameter, (i,j) means that the sum is over pairs of molecules at sites i and j, and $\mathbf{\Omega}_i$ is the symmetric traceless quadrupole tensor associated with a molecule at site i. In general, $\mathbf{\Omega}_i$ may be written in terms of the direction cosines or Euler angles which connect the laboratory and molecular frames. From the traceless condition, we write the eigenvalues, $\Lambda_1 = -1 + \Delta$, $\Lambda_2 = -1 - \Delta$, and $\Lambda_3 = 2$, of the tensor Ω, where Δ is a parameter that gauges the degree of biaxiality [20]. The relation between Δ and molecular anisotropy is made explicit in the Appendix.

The problem is considerably simplified if we resort to a discretization of directions, which has been used to describe the isotropic-nematic transition [17]. We then assume that the principal molecular axes are restricted to the directions of the Cartesian coordinates of the laboratory. Therefore, the

*apvieira@if.usp.br

quadrupole tensor $\mathbf{\Omega}$ can assume only six states, represented by the matrices

$$\begin{pmatrix} -1+\Delta & 0 & 0 \\ 0 & -1-\Delta & 0 \\ 0 & 0 & 2 \end{pmatrix}, \quad \begin{pmatrix} -1+\Delta & 0 & 0 \\ 0 & 2 & 0 \\ 0 & 0 & -1-\Delta \end{pmatrix},$$
$$\begin{pmatrix} -1-\Delta & 0 & 0 \\ 0 & -1+\Delta & 0 \\ 0 & 0 & 2 \end{pmatrix}, \quad \begin{pmatrix} -1-\Delta & 0 & 0 \\ 0 & 2 & 0 \\ 0 & 0 & -1+\Delta \end{pmatrix},$$
$$\begin{pmatrix} 2 & 0 & 0 \\ 0 & -1-\Delta & 0 \\ 0 & 0 & -1+\Delta \end{pmatrix}, \quad \begin{pmatrix} 2 & 0 & 0 \\ 0 & -1+\Delta & 0 \\ 0 & 0 & -1-\Delta \end{pmatrix}, \tag{2}$$

which leads to the definition of the MS6 model. If the molecules are intrinsically uniaxial ($\Delta = 0$), we regain a three-state model, which has been used to describe the transition from the isotropic to the uniaxial nematic phase [17] and to investigate the existence of a biaxial nematic phase in a binary mixture of cylinders and disks [13–15].

The thermodynamic behavior of the MS6 model is determined from the canonical partition function

$$Z = \sum_{\{\mathbf{\Omega}_i\}} \exp\left[\beta\epsilon \sum_{(i,j)} \sum_{\alpha=1,2,3} \Omega_i^{\alpha\alpha}\, \Omega_j^{\alpha\alpha}\right], \tag{3}$$

where $\beta\epsilon = 1/T$, so that T is the temperature in suitable units, and the first sum is over all microscopic configurations $\{\mathbf{\Omega}_i\}$ of this MS6 model. This problem is further simplified if we consider a fully connected model, with equal interactions between all pairs of sites. At this mean-field level, if $\Delta = 0$, we anticipate just a first-order transition between an isotropic and a uniaxial nematic phase. If $\Delta \neq 0$, however, we can describe the transition to a stable biaxial nematic phase.

We now turn to a mixture of intrinsically uniaxial ($\Delta = 0$) and intrinsically biaxial ($\Delta \neq 0$) molecules. In this mixture we have two sets of degrees of freedom: (i) orientational degrees of freedom, $\{\mathbf{\Omega}_i\}$, of a quadrupolar nature, and (ii) shape-disordered degrees of freedom, $\{\Delta_i\}$, with either $\Delta_i = 0$ or $\Delta_i = \Delta \neq 0$, at all lattice sites. These two sets of degrees of freedom may be associated with quite different relaxation times, which leads to the distinction between annealed and quenched situations [18,24]. In the quenched case, the "shape-disordered" degrees of freedom never reach thermal equilibrium during the experimental times. Given a configuration $\{\Delta_i\}$, we calculate a partition function, $Z = Z(\{\Delta_i\})$, and a configuration-dependent free energy, $f(\{\Delta_i\})$. The free energy of the system is the average of $f(\{\Delta_i\})$ over the shape-disordered degrees of freedom, and the concentration of intrinsically biaxial molecules is not a true variable of equilibrium thermodynamics. In the annealed case, the two sets of degrees of freedom are supposed to thermalize during the experimental time, so that the concentration and chemical potential are thermodynamically conjugate variables. In the annealed case, given the concentration, both types of particles are free to move across the system in order to minimize the free energy. In this work, we consider annealed disorder only, which is more appropriate to a liquid-crystalline system.

In the annealed case, consider a binary mixture of N_1 intrinsically biaxial molecules ($\Delta \neq 0$) and $N_2 = N - N_1$ uniaxial molecules ($\Delta = 0$). Given the numbers of uniaxial and biaxial molecules, the canonical partition function is a sum over the orientational and disorder configurations,

$$Z_a = \sum_{\{\mathbf{\Omega}_i\}} {\sum_{\{\Delta_i\}}}' \exp\left[\beta\epsilon \sum_{(i,j)} \sum_{\alpha=1,2,3} \Omega_i^{\alpha\alpha}(\Delta_i)\, \Omega_j^{\alpha\alpha}(\Delta_j)\right], \tag{4}$$

where the prime in the second sum indicates the restriction

$$\sum_{i=1}^{N} \Delta_i = N_1 \Delta. \tag{5}$$

At this stage, in order to deal with the restricted sum in Eq. (4), it is convenient to introduce a chemical potential and change to a grand ensemble. First, we redefine the shape variable of molecule i such that

$$\Delta_i = n_i \Delta, \tag{6}$$

where

$$n_i = \begin{cases} 0 & \text{for a uniaxial object,} \\ 1 & \text{for a biaxial object.} \end{cases} \tag{7}$$

Then the grand partition function is given by

$$\Xi_a = \sum_{\{\mathbf{\Omega}_i\}} \sum_{\{n_i\}} \exp\left[\beta\epsilon \sum_{(i,j)} \sum_{\alpha=1,2,3} \Omega_i^{\alpha\alpha}(n_i)\, \Omega_j^{\alpha\alpha}(n_j) + \beta\mu \sum_i n_i\right], \tag{8}$$

where μ is the chemical potential, which controls the number of biaxial molecules. We remark that the sums over configurations in Eq. (8) are no longer restricted, which makes it possible to carry out the calculations in the mean-field limit, as detailed in the next section.

III. MEAN-FIELD CALCULATIONS

The mean-field version of the MS6 model is given by the Hamiltonian

$$\mathcal{H}_{\mathrm{MF}} = -\frac{\epsilon}{2N} \sum_{i,j=1}^{N} \sum_{\alpha=1}^{3} \Omega_i^{\alpha\alpha}(n_i)\, \Omega_j^{\alpha\alpha}(n_j)$$
$$= -\frac{\epsilon}{2N} \sum_{\alpha=1}^{3} \left[\sum_{i=1}^{N} \Omega_i^{\alpha\alpha}(n_i)\right]^2. \tag{9}$$

The grand partition function Ξ_a in Eq. (8) can be factorized using three Gaussian identities,

$$\exp\left[\frac{\beta\epsilon}{2N}\left(\sum_{i=1}^{N} \Omega_i^{\alpha\alpha}(n_i)\right)^2\right]$$
$$\propto \int_{-\infty}^{+\infty} dq_\alpha \exp\left[-\frac{\beta\epsilon N}{2} q_\alpha^2 + \beta\epsilon q_\alpha \sum_{i=1}^{N} \Omega_i^{\alpha\alpha}(n_i)\right], \tag{10}$$

with $\alpha \in \{1,2,3\}$. This factorization effectively decouples the problem of calculating the grand partition function, and the

sums over $\{\mathbf{\Omega}_i\}$ and $\{n_i\}$ can be performed in a straightforward way, so that we can write

$$\Xi_a \propto \int_{-\infty}^{+\infty} dq_1 \int_{-\infty}^{+\infty} dq_2 \int_{-\infty}^{+\infty} dq_3 \exp(-N\beta\epsilon\psi), \quad (11)$$

where ψ is a functional of $\{q_\alpha\}$. In the thermodynamic limit, the integral can be calculated by standard saddle-point techniques. Thermodynamic equilibrium is then associated with the minimization of ψ with respect to $\{q_\alpha\}$, from which we obtain self-consistent mean-field equations for these quantities. These equations show that $q_1 + q_2 + q_3 = 0$, which suggests the introduction of a symmetric traceless tensor,

$$\mathbf{Q} = \begin{pmatrix} q_1 & 0 & 0 \\ 0 & q_2 & 0 \\ 0 & 0 & q_3 \end{pmatrix}, \quad (12)$$

as an appropriate thermal average of $\mathbf{\Omega}_i(n_i)$. Using the traceless condition, it is convenient to rewrite $\mathbf{Q}$ as

$$\mathbf{Q} = \frac{1}{2}\begin{pmatrix} -S-\eta & 0 & 0 \\ 0 & -S+\eta & 0 \\ 0 & 0 & 2S \end{pmatrix}, \quad (13)$$

in terms of two scalar parameters, S and η [25]. The isotropic phase is given by $S = \eta = 0$. The nematic uniaxial phase is given by $S \neq 0$ and $\eta = 0$ (or $\eta = \pm 3S$). In the biaxial phase, we have $S \neq 0$ and $\eta \neq 0$.

In the following paragraphs we write explicit expressions for the thermodynamic potentials of the uniform system and of the annealed binary mixture. From these expressions, it is easy to perform numerical calculations to draw a plethora of global phase diagrams in terms of the model parameters. In order to asymptotically check the numerical findings, and to make contact with established phenomenological results, we may also write an expansion of the thermodynamic potential in terms of the invariants of the tensor order parameter, $I_n = \mathrm{Tr}\,\mathbf{Q}^n$, with $n = 1,2,\ldots$. Due to the symmetry properties of $\mathbf{Q}$, all these invariants can be written as polynomials depending on two basic invariants, given by

$$I_2 = \mathrm{Tr}\,\mathbf{Q}^2 = \tfrac{1}{2}(3S^2 + \eta^2) \quad (14)$$

and

$$I_3 = \mathrm{Tr}\,\mathbf{Q}^3 = \tfrac{3}{4}S(S^2 - \eta^2). \quad (15)$$

Therefore, the usual form of the Landau–de Gennes expansion is written as

$$g = g_0 + \frac{A}{2} I_2 + \frac{B}{3} I_3 + \frac{C}{4} I_2^2 + \frac{D}{5} I_2 I_3 + \frac{E}{6} I_2^3 + \frac{E'}{6} I_3^2 + \cdots. \quad (16)$$

According to this phenomenological expansion [27], there is a Landau multicritical point for $A = B = 0$. In the vicinity of this Landau point, we can establish parametric expressions for the lines of phase transitions between the isotropic and the nematic phases.

We now consider the specific cases of uniform and annealed systems.

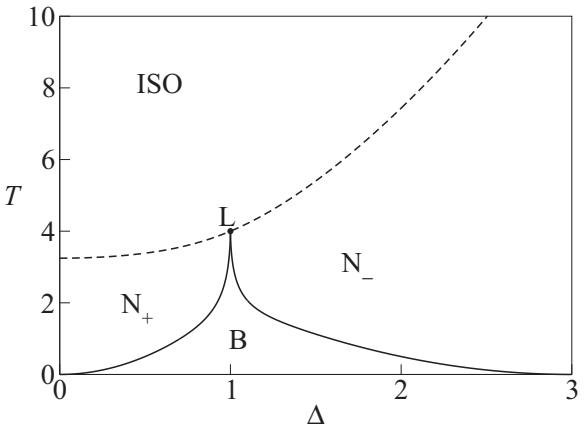

FIG. 1. Phase diagram, in terms of temperature T and degree of biaxiality Δ, for a system of intrinsically biaxial molecules. N_+ and N_- are uniaxial nematic prolate and oblate phases, respectively. B, nematic biaxial phase; L, Landau multicritical point; ISO, isotropic region. Solid lines indicate continuous transitions; dashed lines, first-order phase transitions.

A. Uniform case

Consider a system of intrinsically biaxial molecules ($\Delta_i = \Delta$ for all i). Assuming the discretization of orientations and setting $\mu = 0$ in Eq. (8), since disorder plays no role, the functional ψ is written as

$$\psi = \frac{1}{2}(3S^2 + \eta) - T\ln 2 - T \times \ln\left\{ \exp\left[-\frac{3(S+\eta)}{2T}\right]\cosh\left[\frac{(-3S+\eta)\Delta}{2T}\right] + \exp\left[-\frac{3(-S+\eta)}{2T}\right]\cosh\left[\frac{(3S+\eta)\Delta}{2T}\right] + \exp\left(\frac{3S}{T}\right)\cosh\left(\frac{\eta\Delta}{T}\right)\right\}, \quad (17)$$

where $T = (\beta\epsilon)^{-1}$. Minimizing ψ with respect to S and η leads to the self-consistent mean-field equations, $S = F_1(S,\eta;T,\Delta)$ and $\eta = F_2(S,\eta;T,\Delta)$. The values of S and η at the absolute minimum of ψ correspond to the thermodynamic equilibrium values for a fixed temperature T and degree of biaxiality Δ. The free energy $f = f(T,\Delta)$ of the system is obtained from ψ by inserting the equilibrium values of S and η.

Figure 1 shows the phase diagram in the T-Δ plane, which is obtained by solving the mean-field equations numerically. As should be anticipated from phenomenological arguments, this phase diagram shows two lines of continuous transitions (solid lines) from a biaxial nematic region to the N_+ (prolate) and N_- (oblate) uniaxial nematic regions. These critical lines meet at a Landau multicritical point (L) on the first-order boundary (dashed lines) between the isotropic and the uniaxial nematic phases. It should be remarked that we regain an intrinsically uniaxial system for $\Delta = 3$. The phase diagram for $\Delta > 3$ is mapped onto the region $1 < \Delta' < 3$ by the transformations $\Delta' = (\Delta+3)/(\Delta-1)$ and $T' = 4T/(\Delta-1)^2$. Note that a similar model for asymmetric ellipsoids leads to essentially the same type of phase diagram [7]. Also, a number

of calculations for continuous orientational degrees of freedom lead to the same characteristic topology of this phase diagram (see, for example, the works by Luckhurst and collaborators [9] and Xheng and Palffy-Murhoray [28]).

From the expression of the free energy, we obtain the parameter-dependent coefficients of a Landau–de Gennes expansion about the Landau multicritical point:

$$A = 1 - \frac{3+\Delta^2}{T}, \quad B = \frac{9}{2}\left(\frac{\Delta^2-1}{T^2}\right), \tag{18}$$

$$C = \frac{1}{T^3}\left(\frac{9}{4} + \frac{3}{2}\Delta^2 + \frac{1}{4}\Delta^4\right), \tag{19}$$

$$D = -\frac{45}{16T^4}(\Delta^4 + 2\Delta^2 - 3), \tag{20}$$

$$E = -\frac{1}{480T^5}(41\Delta^6 + 315\Delta^4 + 1215\Delta^2 + 1053), \tag{21}$$

$$E' = \frac{1}{40T^5}(\Delta^6 + 225\Delta^4 - 405\Delta^2 + 243). \tag{22}$$

Therefore, the Landau point (L) is located at $T_L = 4$ and $\Delta_L = 1$. In the vicinity of the Landau point, limiting ourselves to first-order terms in $(T-4)$ and $(\Delta-1)$, we have $A = (1/4)(T-4) - (1/2)(\Delta-1)$, $B = (9/16)(\Delta-1)$, $C = 1/16$, $D = 0$, $E = -41/7680$, and $E' = 1/640$. The sign of E' indicates the stability of the biaxial nematic phase near the Landau point [19,27]. In this mean-field scenario, at fixed $\Delta \neq 1$, as the temperature decreases from a sufficiently high value, the system goes from an isotropic phase to a uniaxial nematic phase and then to a biaxial nematic phase, according to the prediction in the early work by Freiser [5]. It should be remarked that the phenomenological Landau parameters are written in terms of the parameters of the underlying molecular model, which makes it easier to investigate a large range of values.

B. Annealed disorder

In the annealed case, we calculate ψ, given by Eq. (11), in terms of the proper thermodynamic field variables, temperature T, and chemical potential $\mu = \epsilon T \ln z$, where z is the fugacity. For the fully connected MS6 model of a binary mixture of uniaxial and biaxial molecules, the functional ψ is given by

$$\psi = \tfrac{1}{2}(3S^2 + \eta^2) - T\ln 2 - T\ln\sigma, \tag{23}$$

where

$$\begin{aligned}\sigma = {} & e^{-\frac{3(S+\eta)}{2T}}\left\{1 + z\cosh\left[\frac{(3S-\eta)\Delta}{2T}\right]\right\} \\ & + e^{\frac{-3(S-\eta)}{2T}}\left\{1 + z\cosh\left[\frac{(3S+\eta)\Delta}{2T}\right]\right\} \\ & + e^{\frac{3S}{T}}\left\{1 + z\cosh\left(\frac{\eta\Delta}{T}\right)\right\}.\end{aligned} \tag{24}$$

Again, the thermodynamic stable values of S and η are chosen to minimize the function ψ for fixed values of temperature T, degree of biaxiality Δ, and chemical potential μ.

Inserting the equilibrium values of S and η into the expression of ψ, we obtain the grand potential as a function of T, μ, and Δ. If we wish to work with a fixed concentration c of the intrinsically biaxial molecules, the free energy $\phi(c,T;\Delta)$ comes from the definition

$$\phi(c,T;\Delta) = \psi + c\ln z, \tag{25}$$

where the fugacity is eliminated by the expression

$$c = -z\frac{\partial\psi}{\partial z}, \tag{26}$$

and we should insert the equilibrium values of S and η (with the proviso of a Maxwell construction whenever it is necessary).

The grand potential can be used to write a Landau–de Gennes expansion with coefficients

$$A = 1 - \frac{3+z(3+\Delta^2)}{T(1+z)}, \quad B = \frac{9}{2}\frac{z(\Delta^2-1)-1}{T^2(1+z)}, \tag{27}$$

$$C = \frac{9+z[18+9z+6(1+z)\Delta^2-(1-z)\Delta^4]}{4T^3(1+z)^2}, \tag{28}$$

$$D = \frac{15}{16}\frac{9+z[18-6\Delta^2+\Delta^4-3z(-3+2\Delta^2+\Delta^4)]}{T^4(1+z)^2}, \tag{29}$$

$$E = \frac{1053 - z(c_0 + zc_1 + z^2c_2)}{480T^5(1+z)^3}, \tag{30}$$

where

$$c_0 = -3159 - 1215\Delta^2 + 225\Delta^4 - 11\Delta^6, \tag{31}$$

$$c_1 = -3159 - 2430\Delta^2 - 90\Delta^4 + 68\Delta^6 \tag{32}$$

and

$$c_2 = -1053 - 1215\Delta^2 - 315\Delta^4 - 41\Delta^6, \tag{33}$$

$$E' = \frac{243 + z(d_0 + zd_1)}{40T^5(1+z)^2}, \tag{34}$$

where

$$d_0 = 486 - 405\Delta^2 - 45\Delta^4 + \Delta^6 \tag{35}$$

and

$$d_1 = 243 - 405\Delta^2 + 225\Delta^4 + \Delta^6. \tag{36}$$

From the usual condition $A = B = 0$, we locate a Landau multicritical point,

$$\mu_L = -T_L\ln(\Delta^2 - 1), \quad T_L = 4, \tag{37}$$

which requires $\Delta^2 > 1$ and gives an indication of the existence of qualitatively different phase diagrams (as there is no Landau point for $\Delta^2 < 1$).

It is easy to show that this annealed version of the binary mixture exhibits phase diagrams with many distinct topologies. This can be anticipated from an analysis of the energy levels associated with the interaction between molecules, as shown in Fig. 2. In fact, these energy levels are associated with different degrees of degeneracy ω, and some levels cross each other as the biaxiality of the molecules is changed. These degeneracies account for entropic contributions to the free energy, which do affect the equilibrium phase behavior of

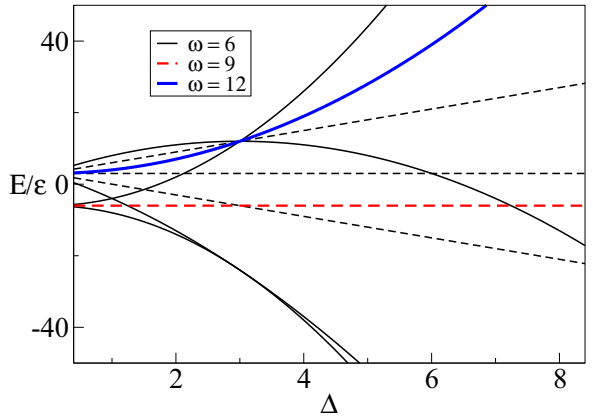

FIG. 2. (Color online) Energy levels as a function of the degree of biaxiality Δ. Level crossings account for variations in the entropic contribution to the free energy. Solid lines correspond to energy levels associated with interactions between two biaxial molecules, while dashed lines indicate energy levels arising from interactions involving at least one uniaxial molecule. Line thickness is proportional to the degeneracy ω of the corresponding level.

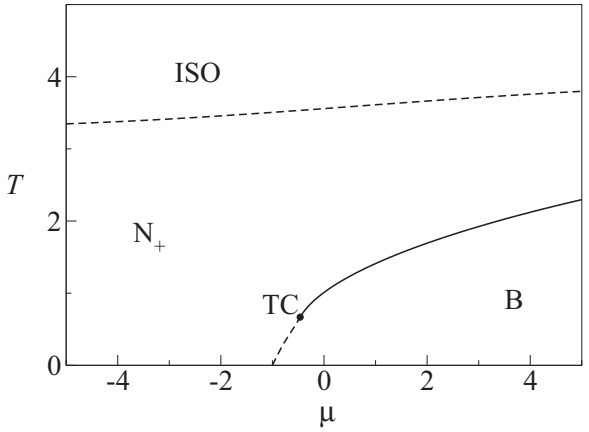

FIG. 3. Phase diagram for a fixed degree of biaxiality $\Delta = 1$, where T is the temperature and μ is the chemical potential. There is a tricritical point (TC) along the boundary separating biaxial (B) and uniaxial (N_+) prolate nematic phases. There is no direct phase transition between the isotropic (ISO) and the biaxial phases (for finite values of the chemical potential).

the system. Therefore, we anticipate qualitative changes in the phase diagrams as Δ assumes values close to the location of the energy level crossings.

Contrary to what is seen in the uniform limit, in the presence of unixial molecules the phase diagrams shown below do not exhibit symmetry between $1 < \Delta \leqslant 3$ and $\Delta > 3$. This is due to the fact that the energy spectrum of the interactions involving uniaxial molecules (shown as dashed lines in Fig. 2) is not invariant under the transformation $\Delta \to (\Delta + 3)/(\Delta - 1)$, $E \to 4E/(\Delta - 1)^2$, contrary to what is observed for the energy spectrum associated with the interactions between a pair of biaxial molecules. In other words, for our choice of interactions the presence of a rod-like solute distinguishes between the biaxial rod-like and the biaxial disk-like components.

We now discuss the various topologies exhibited by the phase diagrams as the biaxiality parameter is changed. Figures 3 and 4 show T-μ and T-c phase diagrams for a fixed degree of biaxiality, $\Delta = 1$, where μ is the chemical potential and c is the concentration of intrinsically biaxial molecules. From the thermodynamic point of view, the first-order boundaries (dashed lines) in the T-μ plane are mapped into coexistence regions [shaded (gray) regions] in the T-c plane. For low temperatures and intermediate concentrations, there is a coexistence region between the uniaxial prolate (N_+) and the biaxial (B) phases. However, at higher concentrations and intermediate temperatures, there is a second-order phase transition (solid line) between the N_+ and the biaxial phase. In fact, the phase diagram exhibits a tricritical point (TC) along the boundary between the N_+ and the biaxial phase. At higher temperatures, there is a first-order phase transition between N_+ and the isotropic (ISO) phase, with a very thin coexistence region, as shown in the inset. Note that an incipient Landau point appears at $c = 1$, which corresponds to an infinite chemical potential, in agreement with the Landau–de Gennes expansion. Phase diagrams with a similar topology (but with no Landau point) can be drawn for $0 < \Delta < 1$.

Figure 5 shows the phase diagram for a fixed degree of biaxiality $\Delta = 1.4$. Similarly to Fig. 4, the N_+ and biaxial (B) phases coexist for intermediate concentrations and low temperatures. However, the system also displays a uniaxial oblate (N_-) nematic phase, which appears at higher concentrations and intermediate temperatures. The biaxial phase appears between the two uniaxial phases, at intermediate temperatures. All three ordered phases become identical to the isotropic (ISO) phase at a Landau multicritical point (L). Also, note that the biaxial phase presents discrete reentrant behavior

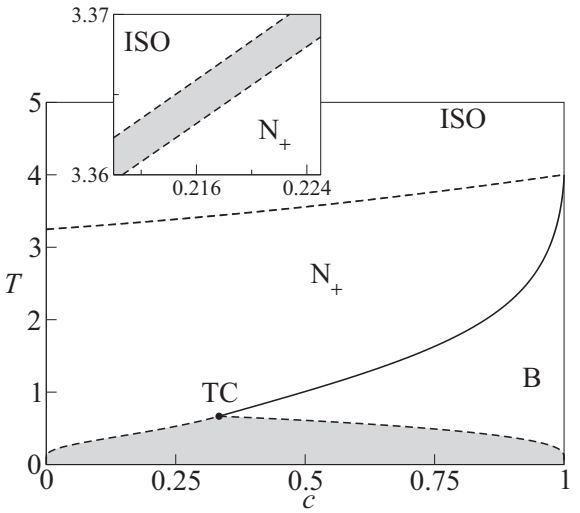

FIG. 4. Phase diagram in terms of the temperature (T) versus the concentration (c) of biaxial molecules, at a fixed degree of biaxiality, $\Delta = 1$. There is an incipient Landau multicritical point at $c = 1$, where the two ordered phases and the isotropic phase become identical. Uniaxial (N_+) and biaxial (B) phases coexist at low temperatures and intermediate concentrations [shaded (gray) region]. The system exhibits a tricritical point (TC) along the boundary of the B phase. Inset: Zoom-in on the coexistence [shaded (gray)] region between the uniaxial nematic and the isotropic phases.

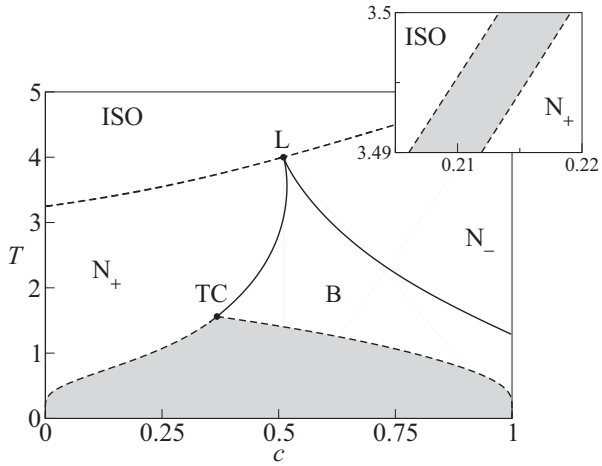

FIG. 5. Phase diagram, in terms of temperature T and concentration c of biaxial (B) molecules, for degree of biaxiality $\Delta = 1.4$. There is a Landau point (L). Note that the B phase displays reentrant behavior near L.

close to the Landau multicritical point. Note that the changes in the topology of the phase diagrams shown in Figs. 4 and 5 are in agreement with the dependence of the energy levels on the degree of biaxiality Δ (see Fig. 2).

The phase behavior of the system changes significantly for a degree of biaxiality around $\Delta = 1.5$, which is close to another crossing of energy levels. For example, in Fig. 6 we show the phase diagram for degree of biaxiality $\Delta = 1.54$. The low-temperature biaxial phase B_- is represented by a tensor order parameter $\mathbf{Q}$, whose largest eigenvalue (in absolute value) is negative. However, an additional biaxial phase (B) appears near the Landau point. The two biaxial phases are stable in disconnected regions of the phase diagram. There is then a coexistence region between the uniaxial nematic phases N_+ and N_-. This region is limited by two critical end points (CE)

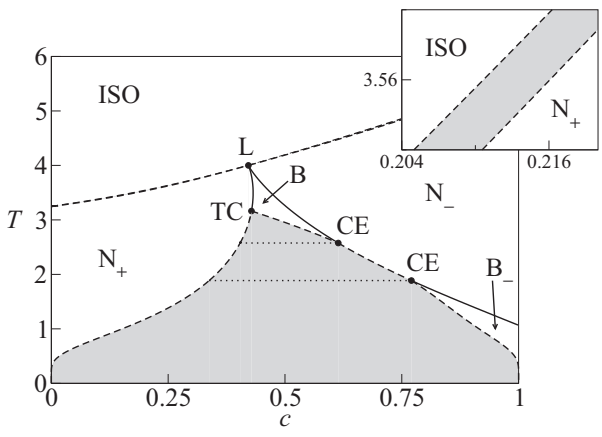

FIG. 6. Phase diagram in the c-T plane for degree of biaxiality $\Delta = 1.54$, where T is the temperature and c is the concentration of biaxial objects. Two nematic biaxial phases are stable in disconnected regions of the phase diagram. There is a coexistence region between the nematic uniaxial phases, ending at two critical end points (CE). Dotted horizontal lines represent special tie lines associated with the CEs.

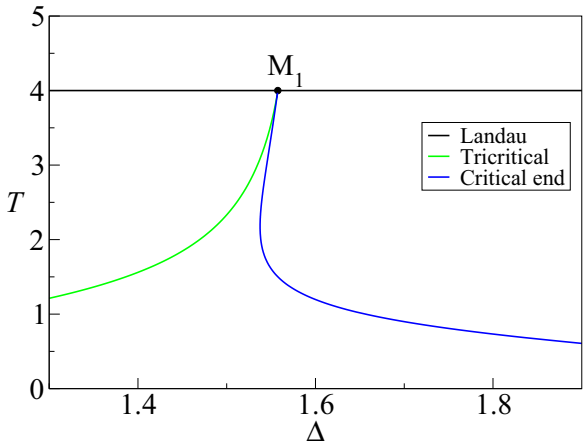

FIG. 7. (Color online) Lines of multicritical points in the Δ-T plane. There is a higher-order multicritical point M_1, at which the lines of Landau points (horizontal black line), tricritical points [left-hand (green) line], and critical end points [right-hand (blue) line] meet. There is then no stable biaxial phase for $\Delta \geqslant \Delta_{M_1}$ in the vicinity of the Landau point.

associated with the biaxial phases. Also, the system exhibits a tricritical point (TC) related to the coexistence region of N_+ and biaxial structures. As in the case $\Delta = 1.4$, shown in Fig. 5, the biaxial phase is reentrant in the vicinity of the Landau point.

The topological changes in the phase diagram can be represented by the projections of the lines of different multicritical points on the T-Δ plane, as indicated in Fig. 7. The temperature of the Landau point (horizontal black line) is a constant function of the degree of biaxiality Δ, which is in agreement with a Landau expansion. The temperature of the tricritical point [left-hand (green) line] increases monotonically with Δ, as suggested by Figs. 4–6. However, the line of critical end points [right-hand (blue) line] presents reentrant behavior in the vicinity of $\Delta = 1.55$, giving rise to the two critical end points, as shown in Fig. 6. All multicritical lines meet at a higher-order multicritical point M_1. Note that the tricritical and high-temperature critical end points are associated with the biaxial phase near the Landau point. As a result, there is no stable biaxial phase in the vicinity of the Landau point for $\Delta \geqslant \Delta_{M_1} \simeq 1.5576$, although the low-temperature biaxial phase survives in a small region at high concentrations and low temperatures. This is illustrated in Fig. 8, for $\Delta = 1.57$. There is no stable biaxial nematic phase close to the Landau point (L), which marks the meeting of various coexistence lines separating the isotropic phase and the two nematic uniaxial phases. Along those lines, there is a coexistence of phases with different values of nematic order parameter S, but the size of the coexistence region tends to vanish as we approach the Landau point.

As the degree of biaxiality is further increased, the system exhibits other distinct phase diagrams, as shown in Figs. 9 and 10. According to Fig. 2, multiple level crossings occur at $\Delta = 3$, which is a strong suggestion of changes in the phase behavior of the system.

Figure 9 shows the phase diagram for $\Delta = 2.9$. A triple point appears, associated with the coexistence of two uniaxial

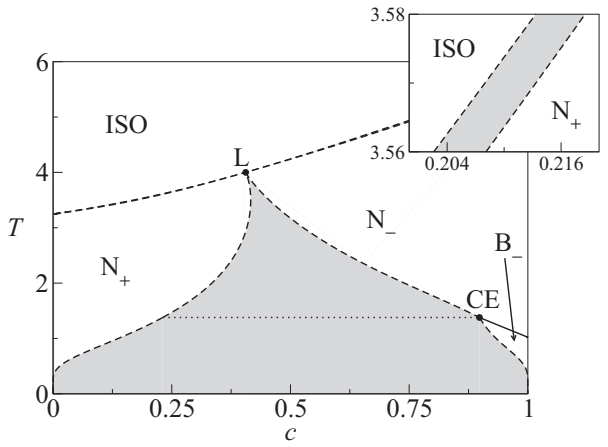

FIG. 8. Phase diagram in terms of temperature (T) versus concentration (c) of biaxial molecules for a fixed degree of biaxiality, $\Delta = 1.57$. The biaxial phase B_- is located at low temperatures and high concentrations. There is no stable B phase near the Landau point (L). The nematic uniaxial phases coexist in a region ending at a critical end point (CE). The dotted horizontal line represents a special tie line associated with the CE.

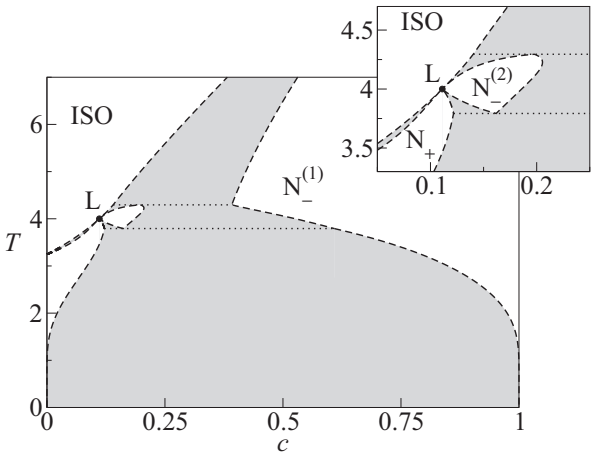

FIG. 10. Phase diagram in terms of temperature T and concentration c of biaxial objects, for degree of biaxiality $\Delta = 3.0$. This system corresponds to a mixture of rods and plates with asymmetric interaction energies. A uniaxial nematic prolate phase, N_+, and two uniaxial nematic oblate phases, $N_-^{(1)}$ and $N_-^{(2)}$, are present. There are two triple points, indicated by the dotted horizontal tie lines.

nematic oblate phases and a uniaxial prolate phase. Also, the coexistence region of uniaxial nematic oblate phases ends at a simple critical point (C). Although it is not shown in Fig. 9, a stable biaxial nematic phase is still present, at low temperatures and high concentrations, as well as the critical end point associated with the biaxial phase.

As Δ is further increased, the simple critical point moves upward in the phase diagram, approaching the lower border of the coexistence region between the uniaxial N_- and the isotropic (ISO) phases. Then the simple critical point is replaced by a second triple point. For example, Fig. 10 represents a phase diagram for $\Delta = 3$. Due to the second triple point, there appears an isolated second uniaxial oblate phase, $N_-^{(2)}$. Note that, according to Eq. (2), the value $\Delta = 3$ corresponds to a binary mixture of rods and plates with asymmetric interaction energies. A symmetric choice of interaction energies [15] presents a much simpler phase diagram, with single nematic uniaxial prolate and oblate phases, in addition to an isotropic phase, and no triple points.

Figures 11 and 12 represent the phase diagrams for $\Delta = 5$ and $\Delta = 6$, respectively. In these diagrams the values of concentrations are conveniently rescaled, so that visual effects are improved. Also, note that we introduce some separations just to emphasize the more interesting sectors of these phase diagrams. There is no stable Landau point in either phase diagram. In Fig. 11, the uniaxial phases N_+ and N_- coexist with the isotropic (ISO) phase at a triple point, and a biaxial B_- phase remains stable at high concentrations. However, in Fig. 12, there is a coexistence region of B_- and isotropic phases, as well as a triple point of coexistence of isotropic, B_-, and N_+ phases. Figures 11 and 12 suggest that the triple

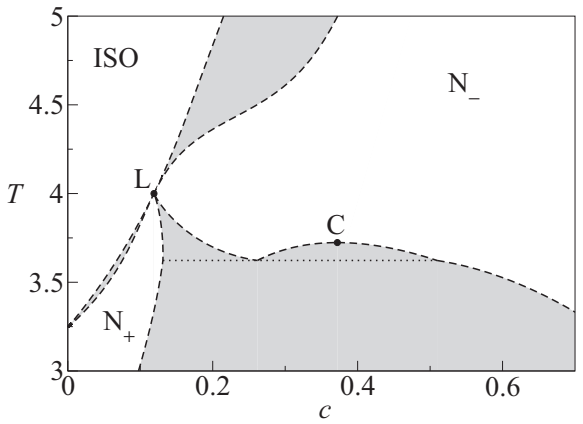

FIG. 9. Phase diagram in terms of temperature T and concentration c of biaxial objects, for degree of biaxiality $\Delta = 2.9$. There is no biaxial nematic phase around the Landau point (L). C indicates the simple critical point associated with a coexistence region between two uniaxial oblate phases. The dotted horizontal line indicates a triple point, corresponding to the coexistence of two uniaxial oblate phase and one uniaxial prolate phase.

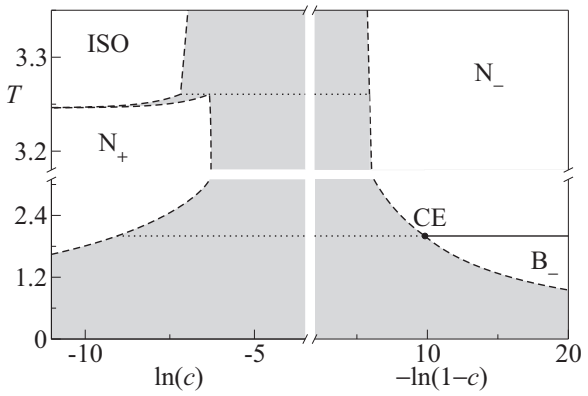

FIG. 11. Phase diagram in terms of temperature T and concentration c of biaxial molecules, for degree of biaxiality $\Delta = 5.0$. The Landau point is absent. A triple point appears, at which N_+, N_-, and ISO phases coexist. The B_- phase is stable at high concentrations.

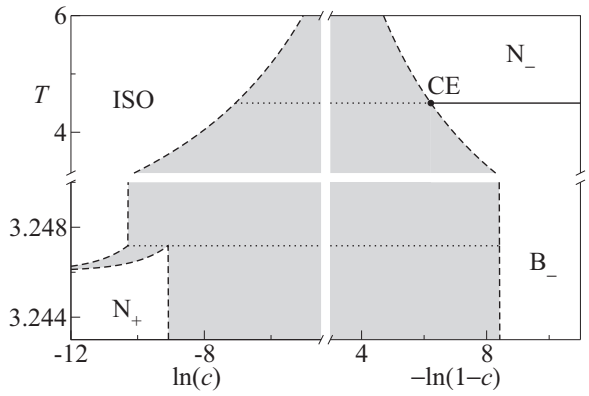

FIG. 12. Phase diagram in terms of temperature T and concentration c of biaxial objects, for degree of biaxiality $\Delta = 6.0$. The Landau point is absent. There is a coexistence region between the ISO and the B_- phases. In addition, ISO, B_-, and N_+ phases coexist at a triple point. The B_- phase is stable at high concentrations.

points meet the critical end point as the degree of biaxiality is increased.

In Fig. 13 we draw the projections of distinct multicritical points on the Δ-T plane. The line of Landau points is still present, as well as the low-temperature part of the line of critical end points associated with B_-. Furthermore, there are lines of triple points associated with the isotropic (ISO) and various nematic uniaxial phases, as depicted in Figs. 9 and 10. The line of Landau points meets the triple lines at another special multicritical point, which we call the Landau end point (LE). This point is characterized by the coexistence of a critical isotropic phase and a noncritical N_- phase. Otherwise, two triple lines meet the line of simple critical points at two multicritical end points (MCE). In addition, for $\Delta \simeq 5.5$, the triple line meets the critical end line at a multicritical point, M_2, where the critical phase N_- coexists with the noncritical N_+ and isotropic phases. Consequently, for $\Delta \geqslant 5.5$, there is a coexistence region between the isotropic and the B_- phases as we increase the concentration of biaxial molecules.

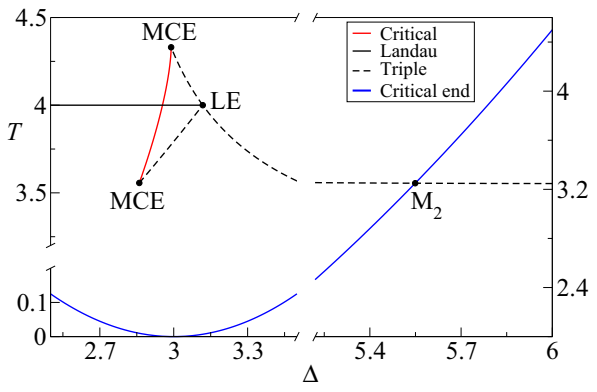

FIG. 13. (Color online) Lines of phase transitions in the Δ-T plane. Dashed black lines represent lines of triple points. The short solid (red) line of simple critical points ends at two multicritical end points (MCE). The line of Landau points meets the lines of triple points at a Landau end point (LE). Also, the longer (blue) line of critical end points crosses the line of triple points at a multicritical point, M_2.

IV. CONCLUSIONS

We have introduced an elementary six-state Maier–Saupe lattice model, which is obtained by the addition of extra degrees of freedom, of a biaxial nature, to an earlier three-state model. We have then described a phase diagram with biaxial as well as uniaxial nematic structures and an isotropic phase. The fully connected MS6 lattice model, of mean-field character, is sufficiently simple to be amenable to a detailed treatment by standard statistical mechanics techniques. Results are obtained in terms of a parameter Δ which gauges the degree of biaxiality. We then use this MS6 model to consider a binary mixture of intrinsically uniaxial ($\Delta = 0$) and intrinsically biaxial ($\Delta \neq 0$) molecules and investigate the effects of "shape variations" on the phase diagrams in terms of temperature and either chemical potential or concentration of biaxial molecules.

Taking into account the fluid character of the liquid-crystalline systems, in the present work we have restricted the analysis to the thermalized (annealed) situation, in which case orientational and shape degrees of freedom reach equilibrium simultaneously. We obtain a wealth of topologically distinct phase diagrams, with several nematically ordered structures and multicritical points.

In the uniform case, in terms of the temperature T and parameter Δ, we regain the first-order transitions between isotropic and uniaxial nematic phases, and the critical lines between the biaxial and the uniaxial nematic phases, which meet at a Landau multicritical point. For a binary mixture of biaxial and uniaxial molecules, we have drawn a number of phase diagrams in terms of the temperature versus concentration of biaxial molecules, with fixed values of Δ, which display many distinct features. Depending on the parameters, additional multicritical points appear, such as tricritical and critical end points associated with the biaxial nematic phase. The Landau, tricritical, and critical end points may give rise to a higher-order multicritical point. Also, depending on the range of values of Δ, there may be a line of Landau points meeting a line of triple points at a Landau end point. This intricate behavior of the mixtures of intrinsically uniaxial and biaxial molecules can be understood in terms of crossings of the microscopic energy levels as we change the degree of biaxiality Δ.

The explicit expressions for the free energy were used to obtain the coefficients of an expansion at high temperatures, in the vicinity of the Landau multicritical point and to make contact with the Landau–de Gennes theory. We were then able to check our numerical findings against a number of phenomenological calculations in the literature. Also, we have provided a simple way of obtaining the expansion coefficients in terms of the values of the molecular parameters.

The calculations predict the presence of stable biaxial nematic phase at low temperatures and sufficiently high concentrations of biaxial molecules, which is in agreement with recent calculations of Longa and coworkers [16] for a more elaborate model system of a mixture of biaxial molecules in the annealed situation. Depending on the degree of biaxiality, we predict first-order transitions between biaxial and uniaxial nematic phases, as well as tricritical points, even in the absence of a Landau multicritical point. For larger values of the degree of biaxiality, the line of Landau points splits into

lines of triple points. Also, we note a clear reentrance of the biaxial regions for some choices of the parameters, which is in agreement with the early work of Alben on a lattice model of platelets [6].

In some recent publications, Akpinar, Reis, and Figueiredo-Neto [29,30] reported x-ray and optical characterizations of biaxial nematic structures in a large class of quaternary liquid-crystalline mixtures. From these measurements, it has been possible to establish many novel phase diagrams in terms of the temperature and molar fraction of the components, which represents a real advance with respect to the early work of Yu and Saupe on a ternary lyotropic mixture. For all concentrations of the amphiphile component, if there is a nematic biaxial structure, it is thermodynamically stable at intermediate temperatures, between regions of different uniaxial nematic structures, at lower and higher temperatures. Also, there are examples of temperature-concentration phase diagrams with a clear indication of the existence of a Landau multicritical point. With a suitable choice of parameters, the MS6 model of binary mixtures can qualitatively reproduce all of these observations. In a very recent experimental investigation, Amaral and coworkers [31] reanalyzed the phase diagram of a ternary sodium dodecyl sulfate lyotropic mixture and pointed out the peculiar coexistence of uniaxial and biaxial nematic structures, which still seems to demand a theoretical explanation.

The present calculations, for the elementary MS6 lattice model at the mean-field level, are a contribution to the understanding of the effects of shape variations on the thermodynamic behavior of complex liquid-crystalline systems. The model of a binary mixture is sufficiently simple to produce a number of analytical and numerical results for a wide range of values of the molecular parameters. Also, it seems to be possible to go beyond the mean-field scenario. The use of more powerful techniques may uncover additional aspects of the phase diagrams, in particular, limitations of the mean-field approach at very low and very high concentrations.

ACKNOWLEDGMENT

We thank the anonymous referee for useful suggestions. We also acknowledge the financial support of the Brazilian agencies FAPESP and CNPq, as well as that of the Brazilian research funding programs INCT and NAP on Complex Fluids.

APPENDIX: RELATION BETWEEN THE BIAXIALITY PARAMETER Δ AND THE MOLECULAR ANISOTROPY

Consider a mesogen which, in a schematic, can be represented by a rectangular parallelepiped with mass m and edges of lengths a, b, and c. The elements of a "traceless inertia tensor" $\mathbf{\Lambda}$ for this object can be defined as

$$\Lambda_{ij} = I_{ij} - \tfrac{1}{3}\delta_{ij}\mathrm{Tr}\,\mathbf{I},$$

where δ_{ij} is the Kronecker delta and $\mathbf{I}$ is the inertia tensor.

In diagonal form, $\mathbf{\Lambda}$ can be written as

$$\mathbf{\Lambda} = \begin{pmatrix} \lambda_1 & 0 & 0 \\ 0 & \lambda_2 & 0 \\ 0 & 0 & \lambda_3 \end{pmatrix},$$

with

$$\lambda_1 = \frac{m}{36}(-2a^2 + b^2 + c^2), \tag{A1}$$

$$\lambda_2 = \frac{m}{36}(a^2 - 2b^2 + c^2), \tag{A2}$$

$$\lambda_3 = \frac{m}{36}(a^2 + b^2 - 2c^2). \tag{A3}$$

Defining

$$\Delta = 3\frac{b^2 - a^2}{a^2 + b^2 - 2c^2},$$

we can rewrite $\mathbf{\Lambda}$ as

$$\mathbf{\Lambda} = \frac{\lambda_3}{2}\begin{pmatrix} -1+\Delta & 0 & 0 \\ 0 & -1-\Delta & 0 \\ 0 & 0 & 2 \end{pmatrix},$$

which is proportional to the first diagonal form of the quadrupole tensor in Eq. (2). The other forms would of course be obtained by the other five configurations in which the parallelepiped oriented so that its edges are always parallel to the Cartesian axis.

Assuming $\lambda_3 < 0$, the choice $a = b < c$ would lead to a "rod-like" uniaxial object and to $\Delta = 0$, whereas $a = c > b$ would correspond to a "disk-like" uniaxial object, with $\Delta = 3$. Both $0 < \Delta < 3$ and $\Delta > 3$ would correspond to unequal edges and, thus, to biaxial objects.

[1] B. R. Acharya, A. Primak, and S. Kumar, Phys. Rev. Lett. **92**, 145506 (2004).
[2] L. A. Madsen, T. J. Dingemans, M. Nakata, and E. T. Samulski, Phys. Rev. Lett. **92**, 145505 (2004).
[3] K. Merkel, A. Kocot, J. K. Vij, R. Korlacki, G. H. Mehl, and T. Meyer, Phys. Rev. Lett. **93**, 237801 (2004).
[4] G. R. Luckhurst, Nature **430**, 413 (2004).
[5] M. J. Freiser, Phys. Rev. Lett. **24**, 1041 (1970).
[6] R. Alben, Phys. Rev. Lett. **30**, 778 (1973).
[7] N. Bocarra, R. Medjani, and L. de Sèze, J. Phys. **38**, 149 (1977).
[8] J. P. Straley, Phys. Rev. A **10**, 1881 (1974).
[9] G. R. Luckhurst, S. Naemura, T. J. Sluckin, K. S. Thomas, and S. S. Turzi, Phys. Rev. E **85**, 031705 (2012).
[10] L. J. Yu and A. Saupe, Phys. Rev. Lett. **45**, 1000 (1980).
[11] R. Berardi, L. Muccioli, S. Orlandi, M. Ricci, and C. Zannoni, J. Phys.: Condens. Matter **20**, 463101 (2008).
[12] Y. Martinez-Ratón and J. A. Cuesta, Phys. Rev. Lett. **89**, 185701 (2002).
[13] E. F. Henriques and V. B. Henriques, J. Chem. Phys. **107**, 8036 (1997).
[14] E. do Carmo, D. B. Liarte, and S. R. Salinas, Phys. Rev. E **81**, 062701 (2010).
[15] E. do Carmo, A. P. Vieira, and S. R. Salinas, Phys. Rev. E **83**, 011701 (2011).
[16] L. Longa, G. Pajak, and T. Wydro, Phys. Rev. E **76**, 011703 (2007).

[17] M. J. de Oliveira and A. M. F. Neto, Phys. Rev. A **34**, 3481 (1986).
[18] S. K. Ma, *Modern Theory of Critical Phenomena* (W. Benjamin, New York, 1976).
[19] P. G. de Gennes and J. Prost, *The Physics of Liquid Crystals* (Oxford University Press, New York, 1993).
[20] As shown in Refs. [21] and [22], the general form of an anisotropic interaction between biaxial molecules involves two biaxiality parameters. For simplicity, here we deal with a special limit which, in the notation of Ref. [23], corresponds to $\lambda = \gamma^2$ and allows us to work with a single biaxiality parameter.
[21] G. R. Luckhurst *et al.*, Mol. Phys. **30**, 1345 (1975).
[22] G. R. Luckhurst and S. Romano, Mol. Phys. **40**, 129 (1980).
[23] A. M. Sonnet, E. G. Virga, and G. E. Durand, Phys. Rev. E **67**, 061701 (2003).
[24] T. A. Witten and P. Pincus, *Structural Fluids: Polymers, Colloids, Surfactants* (Oxford University Press, New York, 2004), Chap. 2.
[25] The parameters S and η introduced in Eq. (13) are, respectively, proportional to the parameters q and η defined in Eqs. (2.68) and (2.69) in Ref. [19]. In our case, comparison between Eqs. (2) and (13) indicates that S ranges from -1 to 2, while η ranges from $\min(-|\pm S-4|, -2-2\Delta-S)$ to $\max(|4\pm S|, 2+2\Delta+S)$. There has actually been a plethora of notations introduced in the last decades to denote second-rank orientational order parameters for biaxial nematics, as reviewed in Ref. [26]. In particular, it can be shown (see p. 746 in Ref. [26]) that our parameters S and η (which are essentially parameters a and b in Ref. [26]) correspond to linear combinations of the four scalar order parameters S, D, P, and C (see Ref. [9]) built from a Cartesian representation of the ordering supertensor. Specifically, our S is built from a linear combination of S and U in Ref. [9], while our η is built from a linear combination of P and C, with the prefactor of C in the combination being proportional to our Δ. (Note that Ref. [26] adopts the notation S, U, P, and F for what are essentially the parameters S, D, P, and C in Ref. [9].)
[26] R. Rosso, Liq. Cryst. **34**, 737 (2007).
[27] E. F. Gramsbergen, L. Longa, and W. H. de Jeu, Phys. Rep. **135**, 195 (1986).
[28] X. Zheng and P. Palffy-Murhoray, Discrete Cont. Dynam. Syst. B **15**, 475 (2011).
[29] E. Akpinar, D. Reis, and A. M. Figueiredo Neto, Eur. Phys. J. E **35**, 50 (2012).
[30] E. Akpinar, D. Reis, and A. M. Figueiredo Neto, Liq. Cryst. **39**, 881 (2012).
[31] L. Q. Amaral, O. R. Santos, W. S. Braga, N. M. Kimura, and A. J. Palangana, Liq. Cryst. **42**, 240 (2015).